

# Three-Dimensional Neutral Transport Simulations of Gas Puff Imaging Experiments

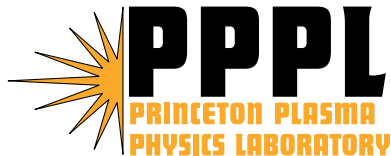
D. P. Stotler, D. A. D'Ippolito<sup>1</sup>, B. LeBlanc, R. J. Maqueda<sup>2</sup>, J. R. Myra<sup>1</sup>,  
S. A. Sabbagh<sup>3</sup>, and S. J. Zweben,

Princeton Plasma Physics Laboratory  
Princeton University  
Princeton NJ 08543

<sup>1</sup>Lodestar Research Corporation, Boulder CO 80301

<sup>2</sup>Los Alamos National Laboratory, Los Alamos NM 87545

<sup>3</sup>Columbia Univ., NY, NY 10027



Note: This poster is available on the Web at:  
<http://w3.pppl.gov/degas2/>

# Gas Puff Imaging (GPI) Experiments Designed to Measure 2-D Structure of Edge Turbulence

---

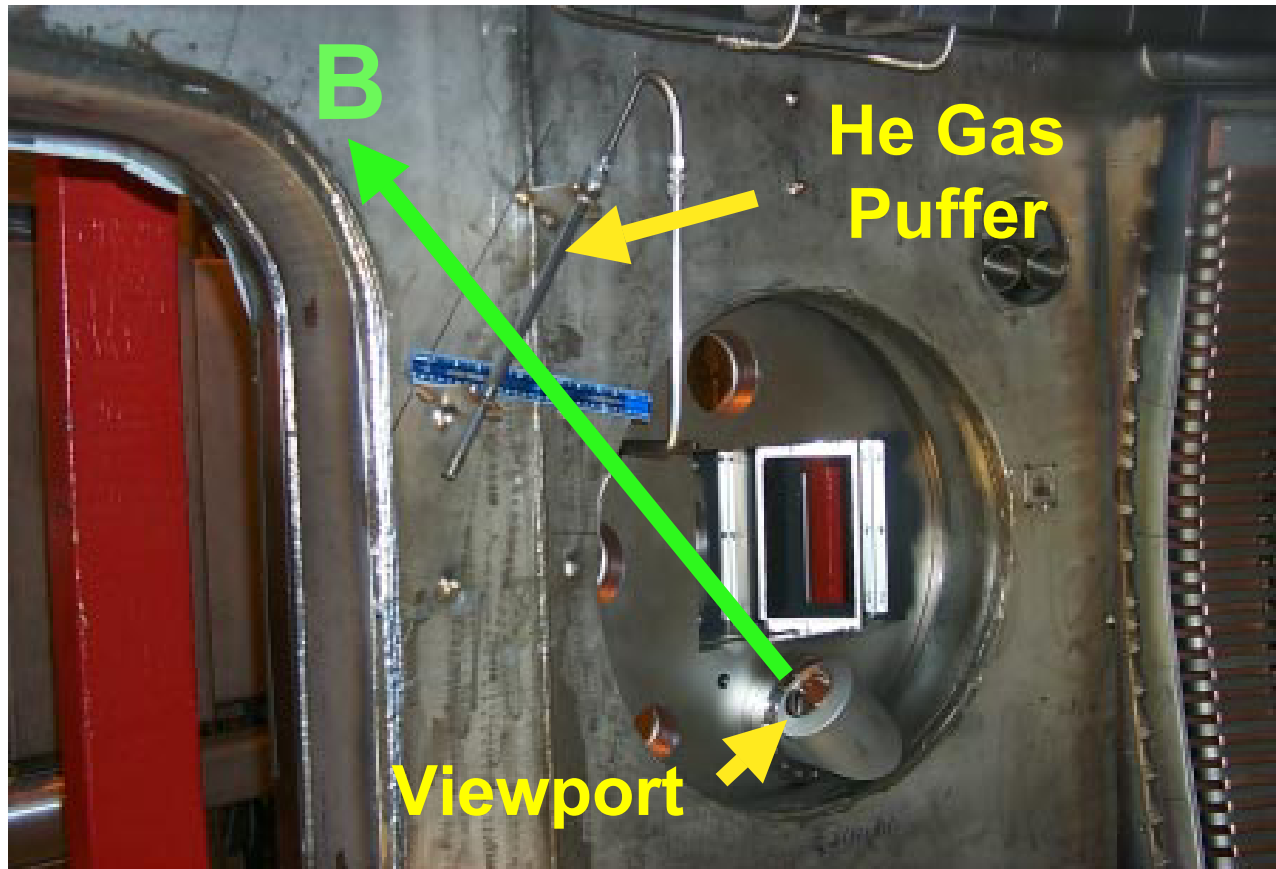
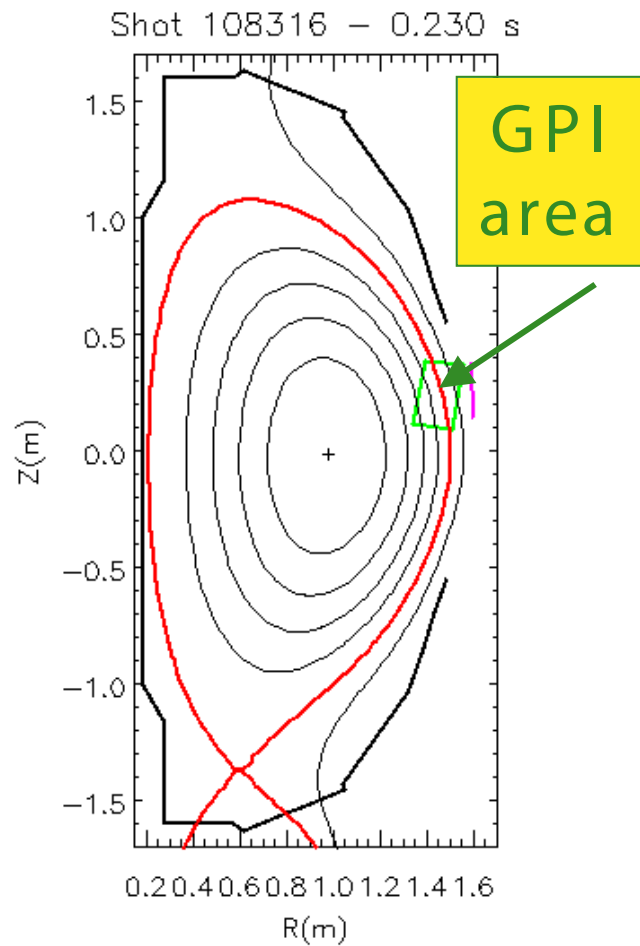
- Puff neutral gas near outer wall,
- View with fast camera fluctuating visible emission resulting from electron impact excitation of that gas,
  - Compare with 3-D nonlinear plasma simulation codes,
  - Reduced theoretical turbulence models,
  - And with turbulence measured by probes.
- NSTX GPI geometry optimizes data quality,
  - But, 3-D arrangement complicates interpretation,
  - $\Rightarrow$  extend DEGAS 2 Monte Carlo neutral transport simulations to 3-D.

# OUTLINE

---

1. Describe GPI experiments,
2. Construction of 3-D DEGAS 2 Simulations,
3. Benchmark code against experiment,
4. Estimate diagnostic resolution,
5. Use neutral density to infer 2-D plasma profiles from GPI images.

# Gas Puff Imaging Hardware Configuration in NSTX



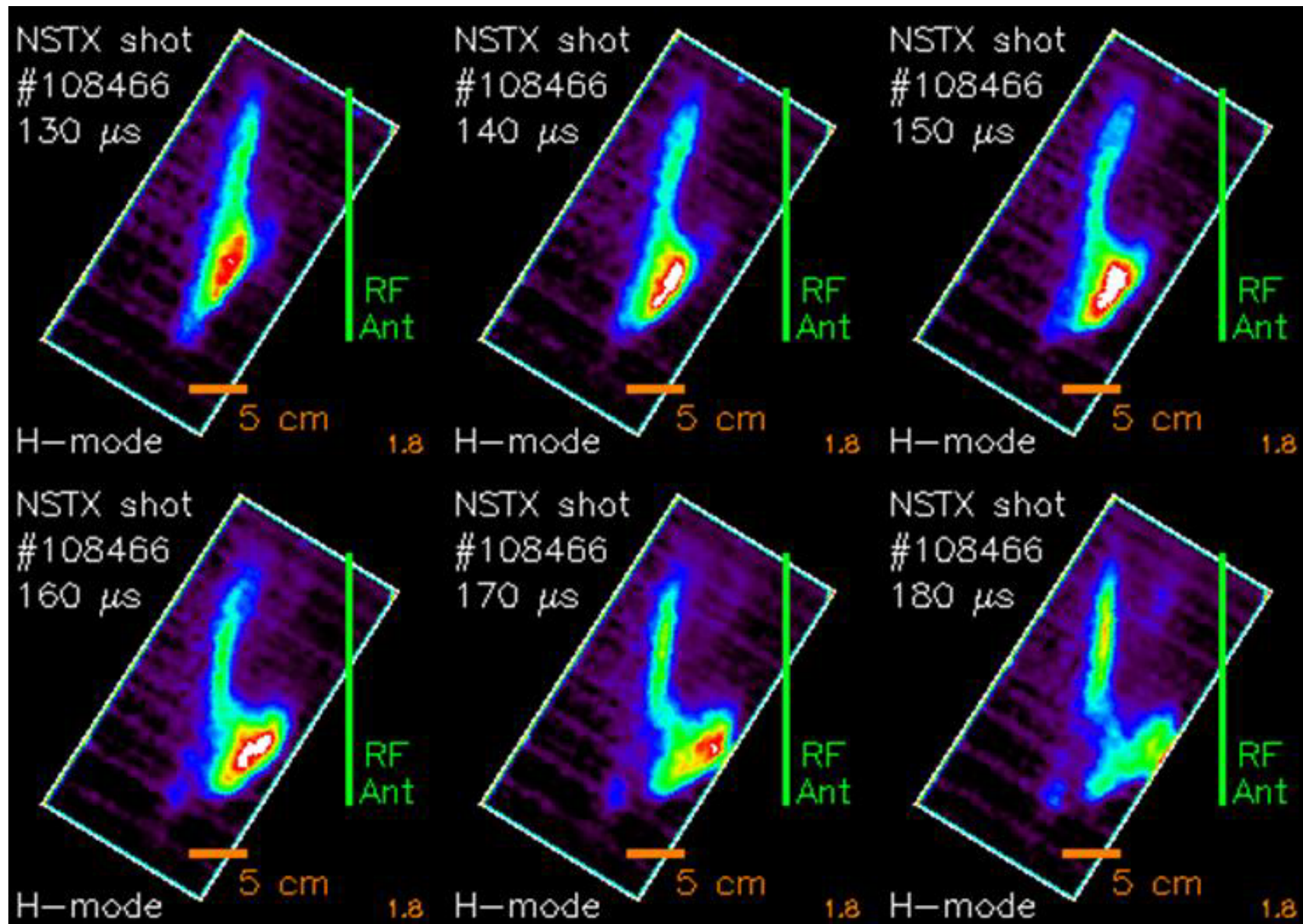
## Experimental Arrangement

---

- NSTX GPI gas puff generated by 30 holes in 30 cm tube  $\perp \vec{B}$ ,
  - $\Rightarrow$  sheet of neutral gas (ideal).
- Camera views 587.6 nm He I line in direction  $\perp$  to sheet &  $\parallel \vec{B}$ .
- Assumes plasma turbulence extended along  $\vec{B}$ ,
  - Shorter scale lengths  $\perp \vec{B}$ ,
  - Supported by theory & observations.

# Camera Records Fluctuating Emission for 28 Frames @10 $\mu$ s/frame

---



## DEGAS 2 Simulation Geometry

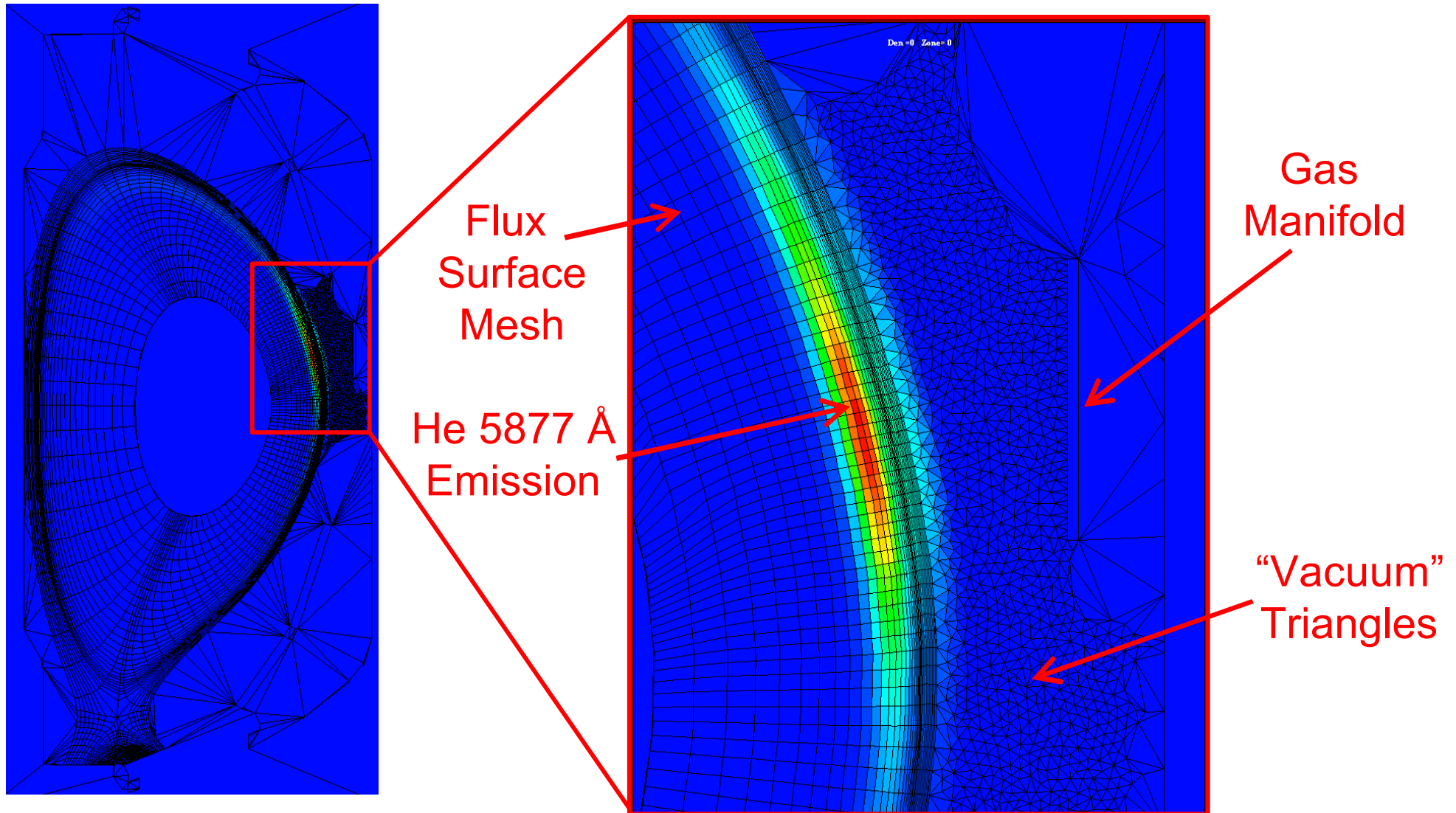
---

- Begin with outline of hardware,
- 2-D plasma mesh defined using EFIT equilibrium,
- Fill remaining volume with triangles,
  - $\Rightarrow$  spatial resolution  $\sim$  few mm.
- Divide into 3-D by  $\phi = \text{constant}$  planes,
  - Width  $0.5^\circ - 1^\circ$  near manifold,
  - Wider near edges,  $\pm 45^\circ$  from manifold.

# Realistic, High Resolution Geometry

## NSTX Shot 108321, 187 ms

---

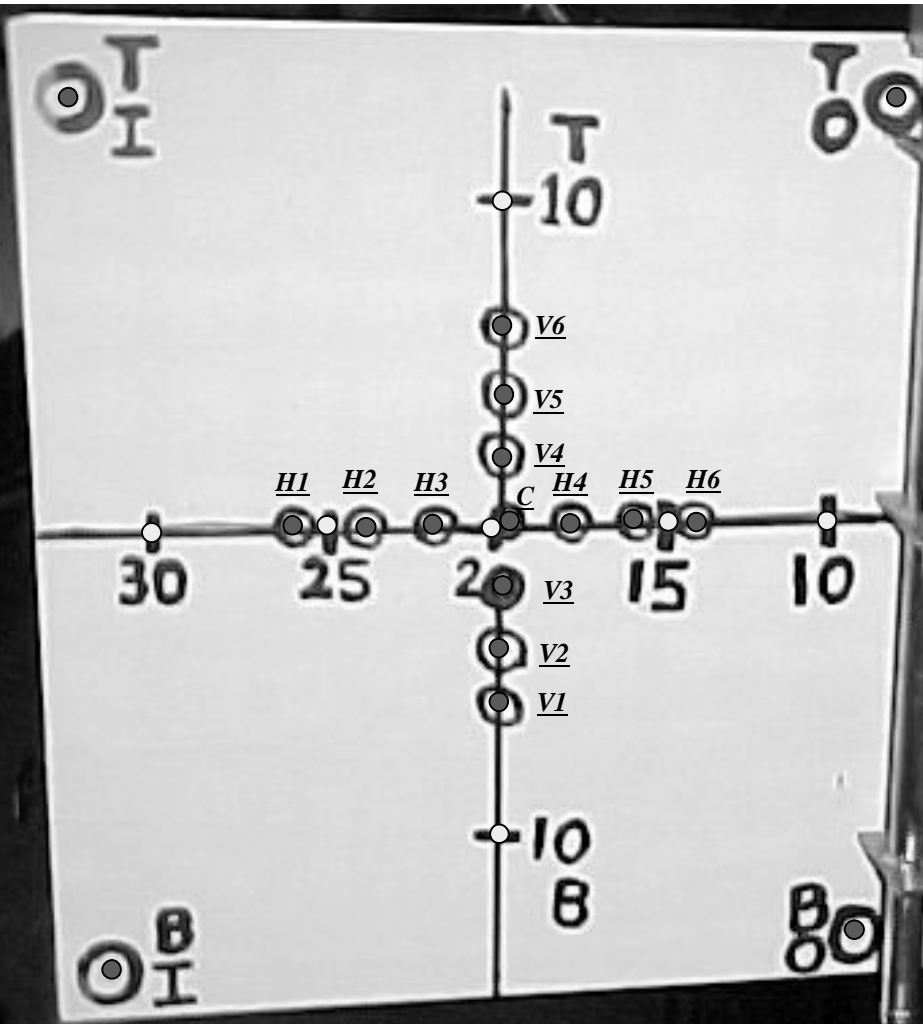


- Gas source simulated in 3-D,
  - Specification of 3-D structures currently limited to toroidal solids of revolution,
  - $\Rightarrow$  manifold is rectangle rotated through  $6^\circ$  in  $\phi$ ,
  - But, source points specified on diagonal line matching actual manifold.
- Limit size by treating only  $R \simeq 1.1 \rightarrow R \simeq 1.7$  m  
&  $Z \simeq -0.2 \rightarrow Z \simeq 0.6$  m.

# GPI Camera Emulation

---

- Directly compute  $81 \times 161$  pixel view of camera,
- Each pixel corresponds to chord integral through problem,
- Chords start at reentrant window,
- Second point is measured 3-D location of intersection with “target plane”.
- Replicate 0.4 cm camera resolution with chords having halfwidth  $0.16^\circ$  at target plane.
- Full resolution images computed during post-processing with MPI.



# Plasma Data

---

- Single-time  $n_e(R_{\text{mid}})$ ,  $T_e(R_{\text{mid}})$  from Thomson scattering,
- Assume  $n_i = n_e(\psi)$ ,  $T_i = T_e(\psi)$  only.
- Simulations are time-independent,
  - Not considering time varying plasma here.

# He Atomic Physics from Goto

---

- He collisional-radiative model from Goto  
⇒ ionization & emission rates,

- Metastable  $2^1S$ ,  $2^3S$  *not* transported,
  - Will consider separately.

- Emission rate given by

$$S = n(1^1S) \frac{n(3^3D)}{n(1^1S)} A_{3^3D \rightarrow 2^3P} \equiv n_0 F(n_e, T_e),$$

- where  $A_{3^3D \rightarrow 2^3P} = 7.1 \times 10^7 \text{ s}^{-1}$ .

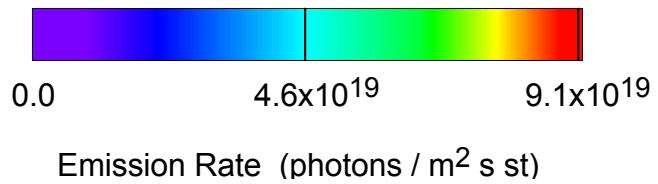
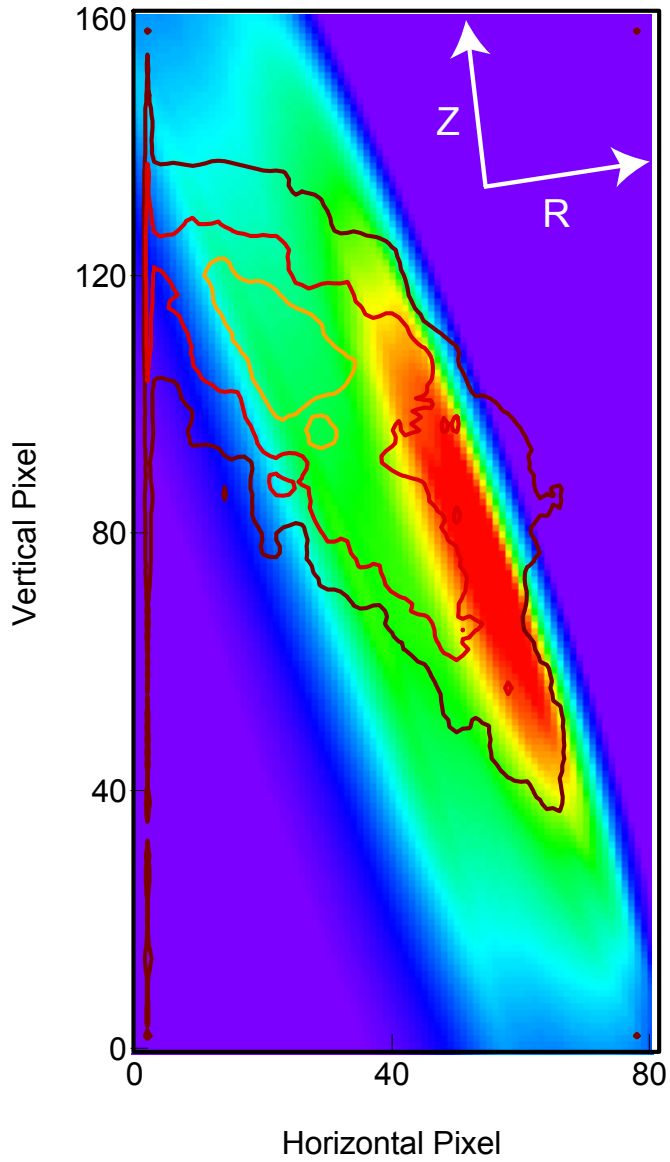
- He + D<sup>+</sup> elastic scattering data from Krstic & Schultz.

# Compare With Experiment

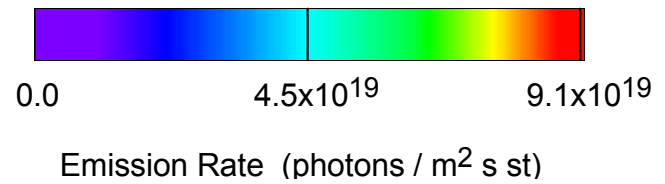
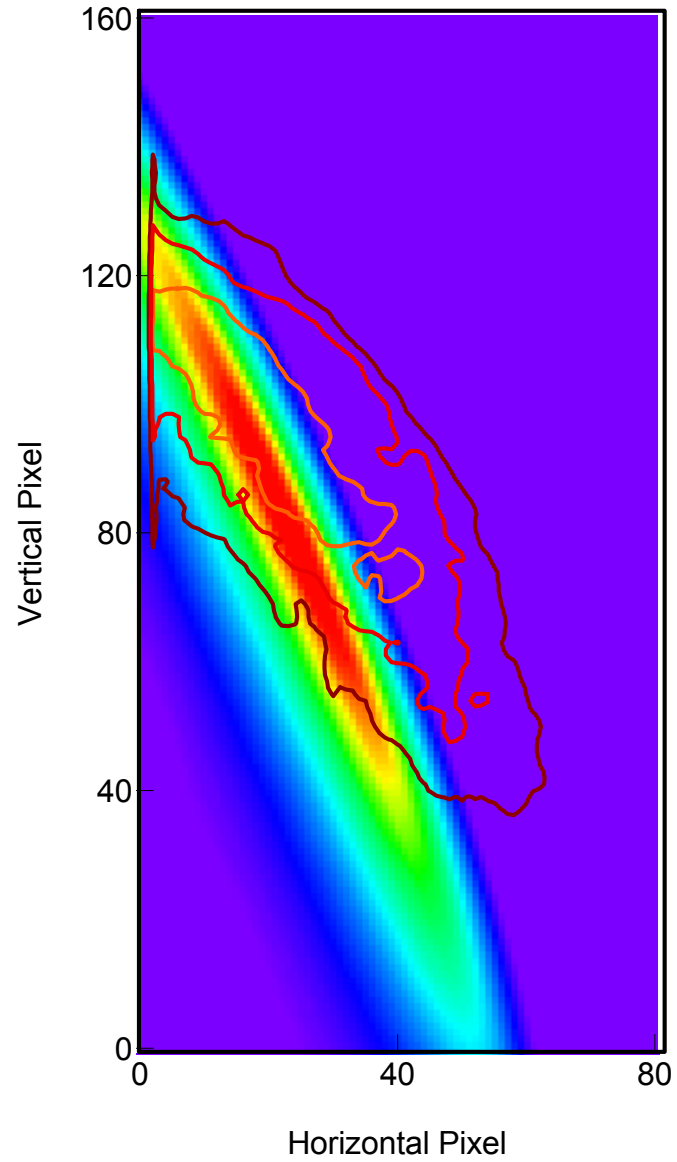
---

- Two shots: 108311 (H-mode), 108322 (L-mode),
- Overlay experimental data,
  - 3-D plasma used in DEGAS 2 *does not* correspond to a particular GPI frame,
  - $\Rightarrow$  compare with “averaged” frame,
  - Use median in time to reduce effects of blobs.
- Middle contour is half-maximum.

108311



108322



# Width Comparison

---

- Half-widths in simulation: 3 mm (108311) & 2 mm (108322),
- Observed: 1 – 2 mm (108311) & 2 – 3 mm (108322),
  - Difficult to define,
  - Examined individual frames as well as median.
- Agreement rough, but qualitatively better than with 2-D simulations.

# Observed & Simulated Cloud Orientations Differ

---

- Experimental & simulated contours angled  $15^\circ$ ,
  - Simulated emission follows flux / plasma contours,
  - Deviation between cloud & separatrix angle noted before.
- Quiescent GPI cloud angles vary  $20^\circ$  shot-to-shot!
- But, EFIT equilibria show flux surface changes of only  $1 - 2^\circ$ !
  - $\Rightarrow$  again, emission *not* aligned with flux surfaces.
- GPI hardware not moved  $\Rightarrow$  can't blame calibration.

- Possible explanations:

1. Plasma parameters varying on flux surfaces,

2. Magnetic equilibrium shapes different from EFIT.

# Radial Resolution Estimate

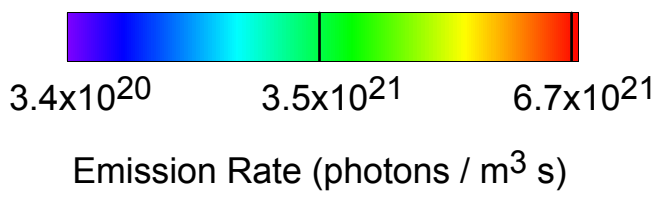
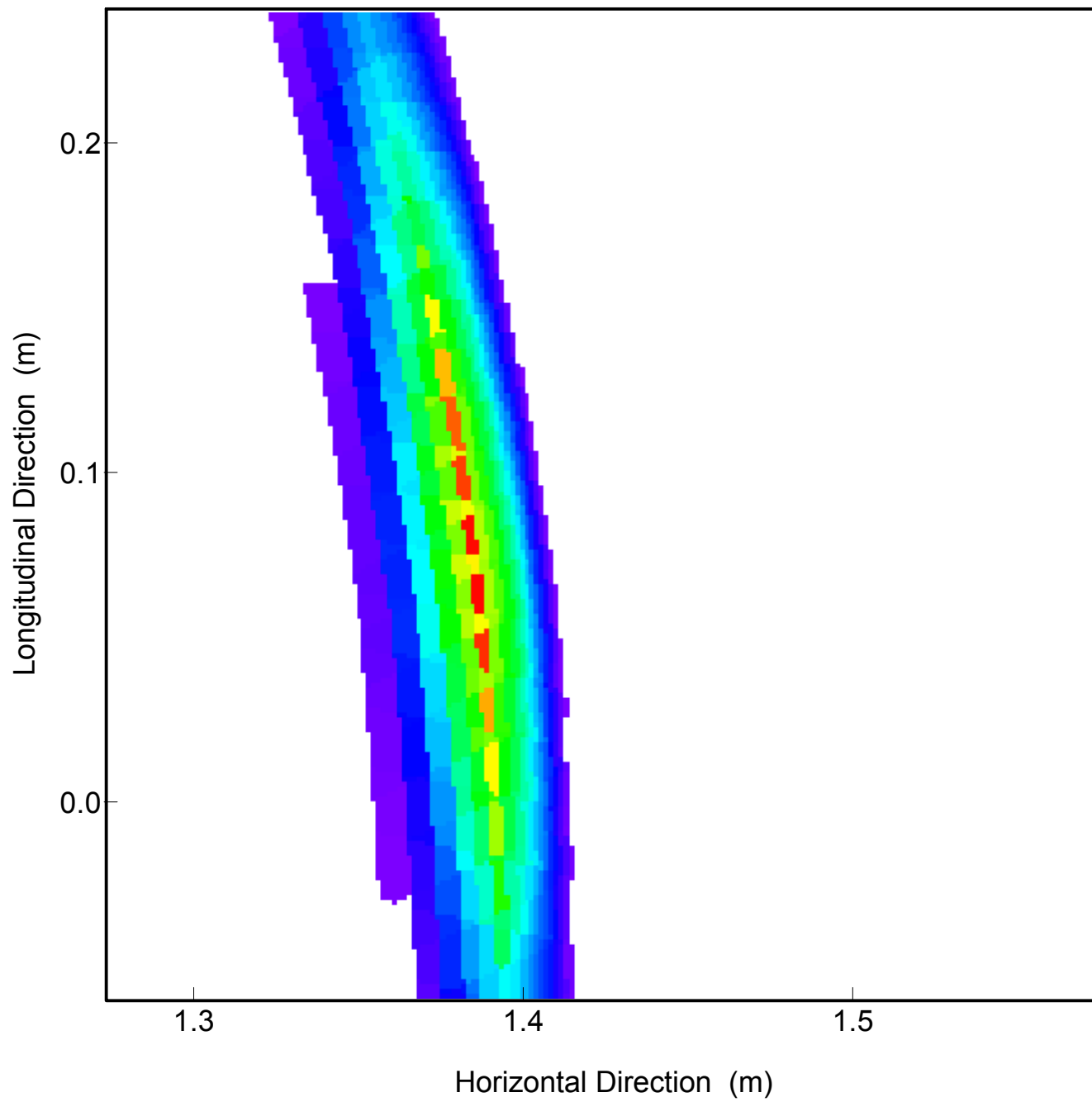
---

- Previous radial resolution estimated  $2 \pm 1$  cm based on toroidal cloud width & degree of camera / field alignment,
  - Effect of latter on poloidal resolution: 0.5 – 2 cm.
- For shots used here  $I_p$  &  $B_T$  match values used in design of GPI  
⇒ can't examine misalignment,
- Check toroidal width with slices along camera view,
  1. FWHM = 25 cm for 108322,
  2. 20 cm for 108311,
  3. Observed: 24 cm.

# Estimate Resolution with Tracer Perturbation

---

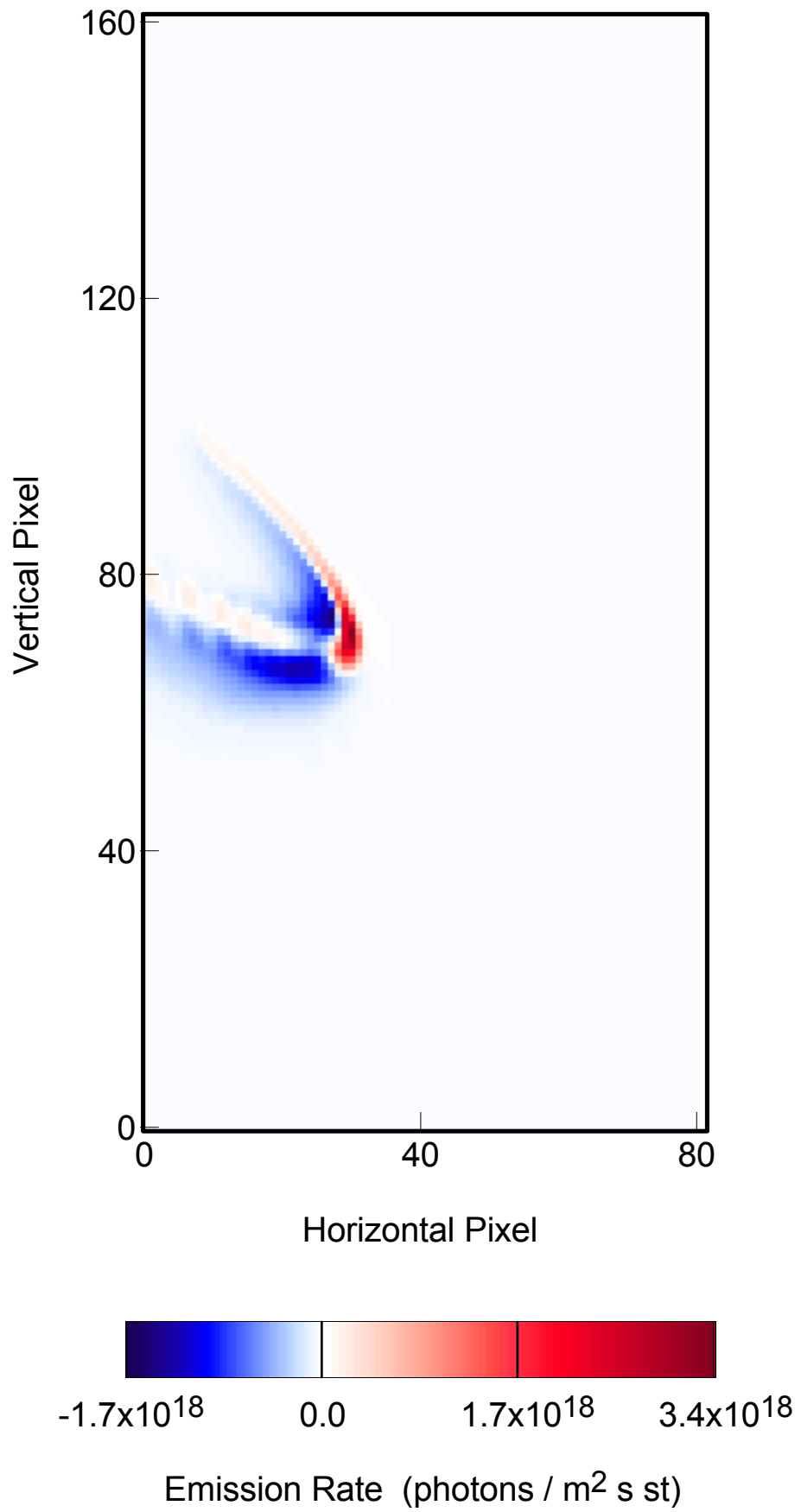
- Estimate effect of cloud width & field line curvature on resolution with “tracer” perturbation:
  - Choose one cell, 0.7 cm wide  $\times$  1 cm tall, from mesh,
  - Define toroidal  $\phi$  mesh using local  $\vec{B}$  pitch so incremental poloidal steps along 2-D mesh can follow field line on either side,
  - Double  $n_e$  everywhere along this path.
- Emission due to perturbation clear in camera-aligned slice,
- Relatively long  $\Rightarrow$  field-camera alignment is indeed good,
- Width  $\perp$  to viewing chord 1.6 cm  $\rightarrow$  initial measure of radial resolution,
  - But, effective resolution smaller since camera integrates along chords.



# Plot Perturbed - Unperturbed Emission

---

- Curved shape  $\leftrightarrow$  field line shape seen by camera,
- Negative values  $\leftrightarrow$  “shadowed” region.
- Radial half-width = 0.6 cm,
- Poloidal half-width = 1.2 cm,
  - $\Rightarrow$  same as size of initial cell!
  - Toroidal extent of cloud *does not* significantly degrade radial resolution (at least here).



# Effective Neutral Density

---

- Use GPI data + DEGAS 2 neutral density to get 2-D  $n_e, T_e$ ,
  - Use to test theories of blob motion,
  - $n_e, T_e \rightarrow \Phi$ ,
  - $\Rightarrow \vec{E} \times \vec{B}$  & motion of blobs.
- GPI  $\Rightarrow S$ ,
- DEGAS 2  $\Rightarrow n_0$ ,
- $F(n_e, T_e)$  known,
- $\Rightarrow$  can invert if we know  $n_e(T_e)$ .

# First Effective Neutral Density

---

- Camera signal for pixel  $i$ :

$$I(i) = \int \frac{dl}{4\pi} F(\vec{x}) n_0(\vec{x}).$$

- $\rightarrow$  2-D function of  $i$ ,
- But, want as function of  $\vec{x}$ .
- Only connection is target plane &  $\vec{x}_i$ ,
  - $\Rightarrow$  best we can do is  $n_e(\vec{x}_i)$  and  $T_e(\vec{x}_i)$ .
- Camera aligned with  $\vec{B}$  & blobs constant on  $\vec{B} \Rightarrow F(\vec{x}) \sim F(\vec{x}_i) = \text{constant}$ ,

$$I(i) \simeq F(\vec{x}_i) \int \frac{dl}{4\pi} n_0(\vec{x}).$$

- Suggests using

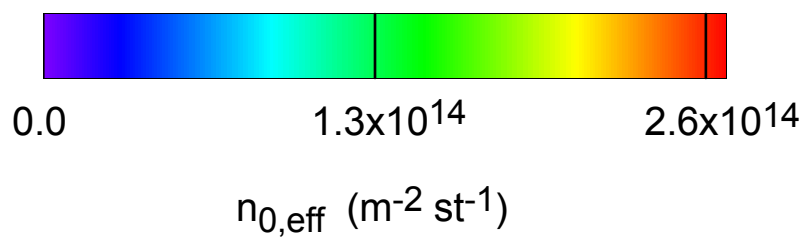
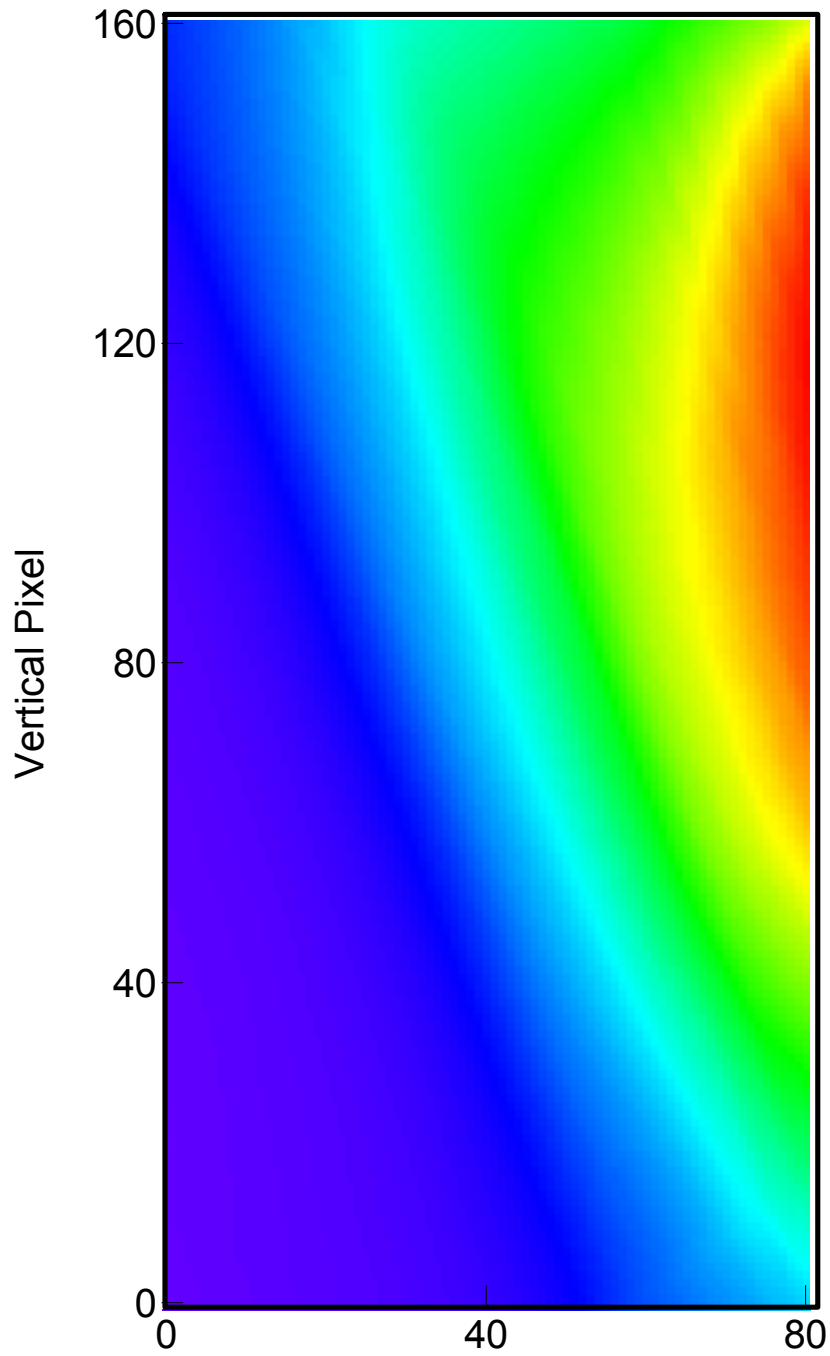
$$n_{0,\text{eff}} \equiv \int \frac{dl}{4\pi} n_0(\vec{x}) \simeq I(i)/F(\vec{x}_i).$$

- GPI data not calibrated  $\Rightarrow$  simulated image needs normalization,
  - But, don't have  $I$  corresponding to DEGAS 2 plasma,
  - *Assume* we can get something that's consistent (e.g., median),
  - $\Rightarrow$  compute

$$\alpha \equiv I_e(i)/I_s(i).$$

- $\alpha$  must be a constant or slightly varying with  $i$ .
- Could then invert frame  $k$ ,

$$F(\vec{x}_i; t_k) = \frac{1}{\alpha} \frac{I_e(i; t_k)}{n_{0,\text{eff}}}.$$



# Second Effective Neutral Density

---

- But, above approximation off by  $\sim$  few,

- To do better:

$$I(i) = \int_{l \in l_0} \frac{dl}{4\pi} F(\vec{x}) n_0(\vec{x}) + \int_{l \notin l_0} \frac{dl}{4\pi} F(\vec{x}) n_0(\vec{x}),$$

where  $l_0 =$  region near target plane.

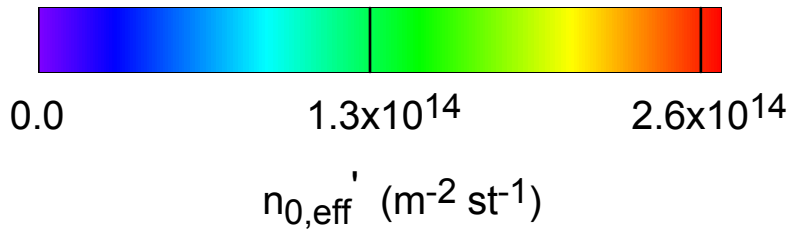
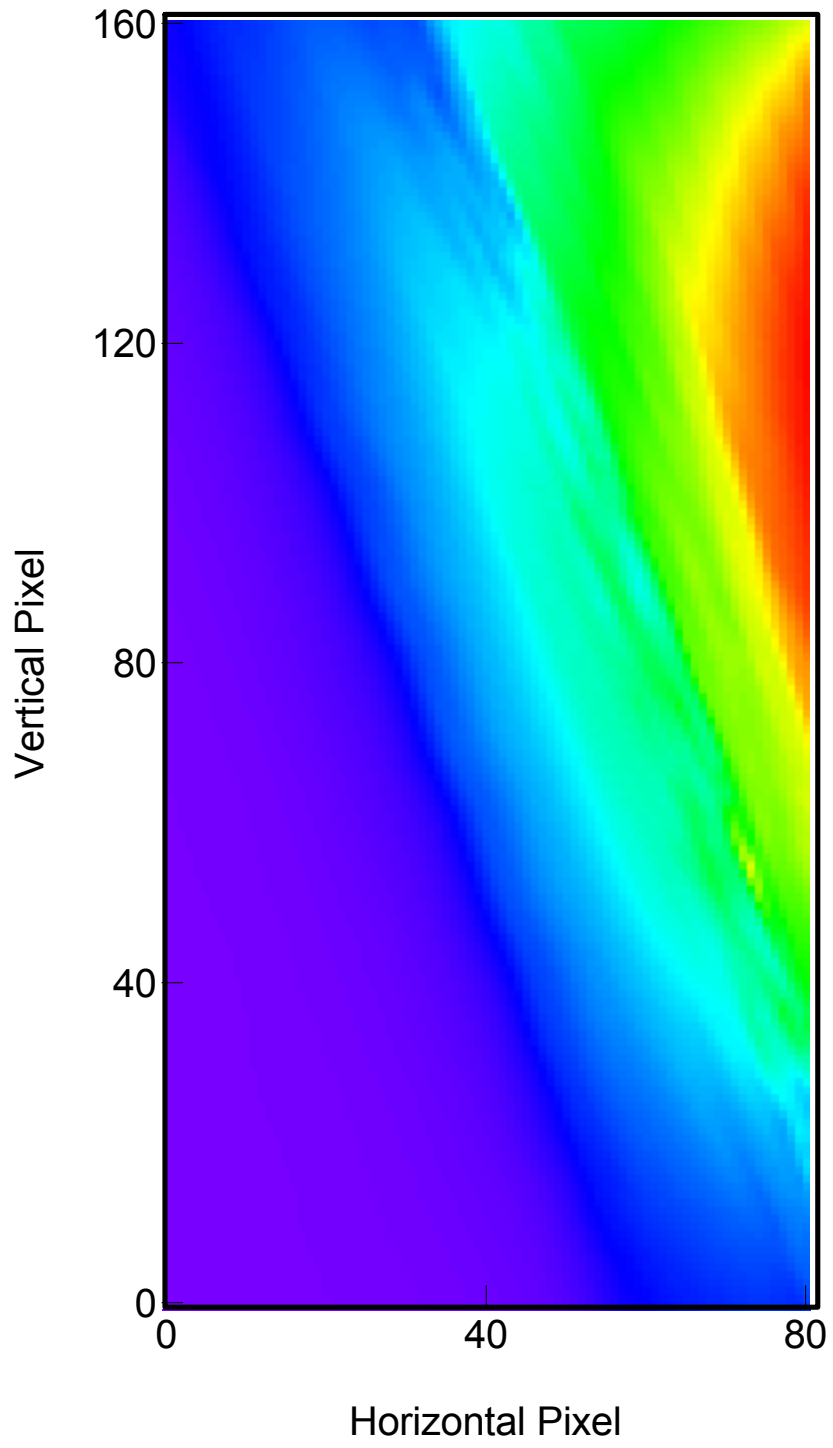
- Assume first part dominates  $\Rightarrow$  try

$$\langle F \rangle(i) \equiv \frac{\int_{l \in l_0} dl F(\vec{x}) n_0(\vec{x}) / 4\pi}{\int_{l \in l_0} dl n_0(\vec{x}) / 4\pi}.$$

- Corresponding effective neutral density:

$$n'_{0,\text{eff}} \equiv I(i) / \langle F \rangle(i).$$

- For small  $l_0$ ,  $\langle F \rangle \simeq F(\vec{x}_i)$ ,
  - $\Rightarrow$  can use above procedure to get  $n_e(\vec{x}_i)$  and  $T_e(\vec{x}_i)$ ,
  - Better accounts for contributions away from target plane.



# Caveats

---

- $l_0$  must cover several computational zones,
  - Or, get noisy results,
  - Hinder calculation of  $n_e$ .
- But, if  $l_0$  too large  $\langle F \rangle \neq F(\vec{x}_i)$ , & cannot associate resulting  $n_e$  with target plane.
- Note that  $n_{0,\text{eff}} \rightarrow n'_{0,\text{eff}}$  when  $l_0 \rightarrow \infty$ .
- In practice, however, simulation & observation differ too much,
  - DEGAS 2  $n_{0,\text{eff}}$  must be shifted & rotated to line up emission clouds,
  - In this case,  $n_{0,\text{eff}}$  and  $n'_{0,\text{eff}}$  work equally well.

# **Theory and Experimental Analysis of Blobs in the NSTX Boundary Plasma\***

***J.R. Myra, D.A. D'Ippolito (Lodestar),  
D.P. Stotler, S.J. Zweben (PPPL),  
R. Maqueda, and the NSTX Team***

\*Work supported by U.S. DOE grants/contract DE-FG03-02ER54678, DE-FG03-97ER54392 and DE-AC02-76CH03073.

prepared for presentation at the PET meeting [Stotler et al.; D'Ippolito et al.]

Sept. 3 - 5, 2003, San Diego, CA

and at the APS/DPP meeting

Oct. 27 - 31, 2003, Albuquerque, NM

# Procedure

## Theory

- Intensity of light emission  $I$  is related to the neutral density  $n_0$ , the plasma density and temperature  $n_e$  and  $T_e$ , and an atomic physics function  $F$  by

$$I = n_0 F(n_e, T_e)$$

- If  $n_0$  is known and the 2D image of intensity  $I$  is measured by the GPI camera, then  $F$  can be inverted for  $n_e$  and  $T_e$  if we assume that  $T_e = T_e(n_e)$ .
- $T_e = T_e(n_e)$  is justified for interchange turbulence when  $E \times B$  turbulent motion passively convects  $n_e$  and  $T_e$  together.
- The mapping  $F^{-1}(I/n_0)$  to  $n_e$  and  $T_e$  is determined from the equilibrium frame using the Thompson (TS) data to calibrate  $I$ .
- On the time and space scales of the turbulence we assume  $n_0 = \text{constant}$ , i.e. calculate  $n_0$  for the equilibrium and use it for the turbulence
- caveat: parallel plasma losses are neglected. Applies for fast moving plasma blobs with  $\tau_{\text{convection}} < \tau_{\parallel}$

*basic idea: measure  $I$  and map to  $n_e$  and  $T_e$   
from a knowledge of  $n_0$*

## Equilibrium calibration

### Goal

- Use the calculated neutral density (not absolutely calibrated), the TS data and an equilibrium GPI frame to construct the mappings  $I \rightarrow n_e, T_e$  that will be used to interpret the turbulent GPI images.
- Here *equilibrium* means quiescent background plasma on which intermittent *blobs* propagate.

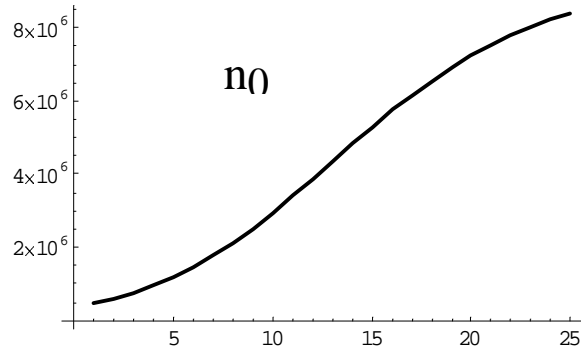
### Neutral density

- calculated from DEGAS-2 using TS profiles and geometry as input
- shifted and rotated so that the calculated emission pattern aligns with the GPI emission image
- fit to a separable function of pseudo-flux coordinates  $(x, y) = (\text{radial}, \text{poloidal})$

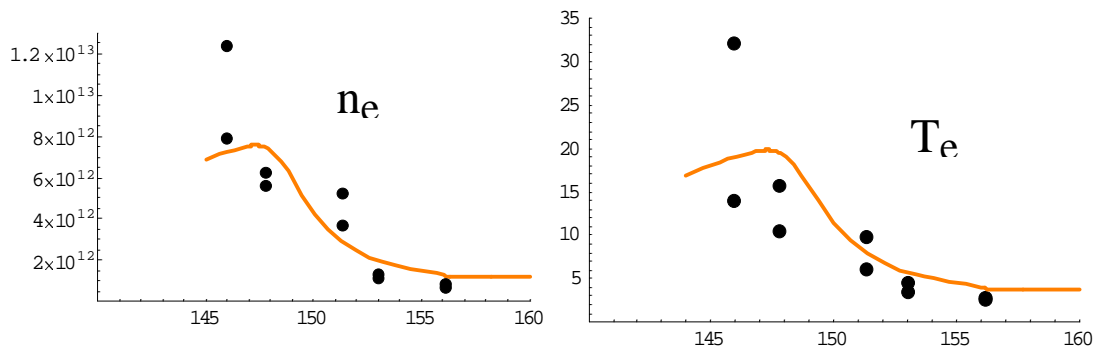
### Equilibrium

- take the time *median* over the 28 frames of the GPI movie as the equilibrium GPI frame
  - median eliminates intermittent objects (blobs) from the equilibrium
- use smooth fits to the TS data projected along field lines to construct the *equilibrium*  $n_e(x), T_e(x)$  profiles

## Sample equilibrium reconstruction



Radial dependence of neutral profile  $n_0(x)$  from DEGAS-2 (arbitrary normalization).



Comparison of reconstructed profiles with TS data. black dots: TS data; orange curve: reconstructed profiles using our procedure on the equilibrium frame.

Reconstruction is not accurate into the core where both  $I$  and  $n_0$  become small. (i.e. one gets  $F = 0/0$ )

# Comparison of $n_e$ and $T_e$ for equilibrium and turbulent frames

## *equilibrium frame*

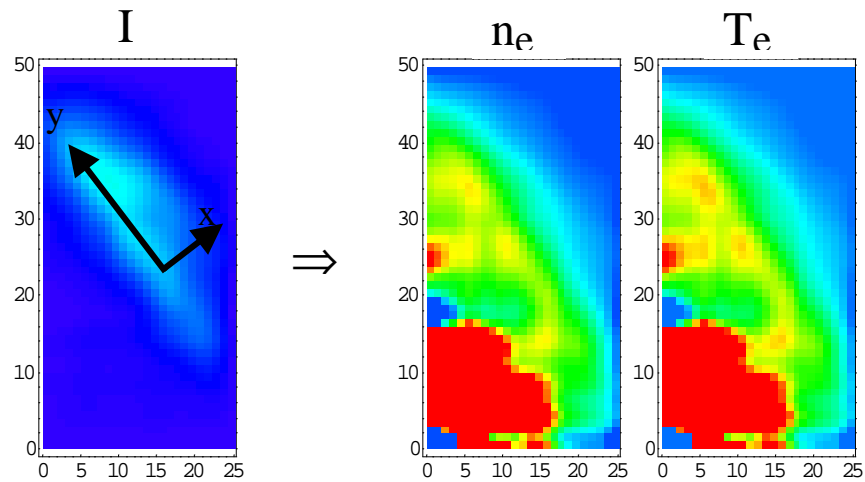
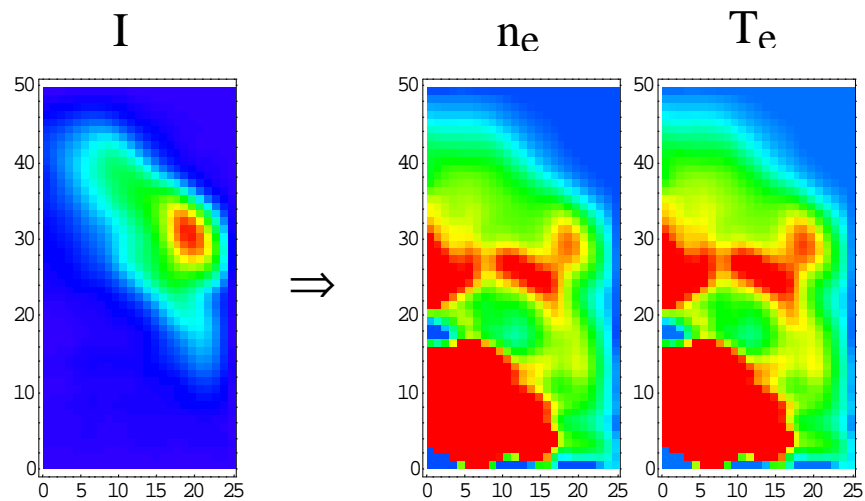
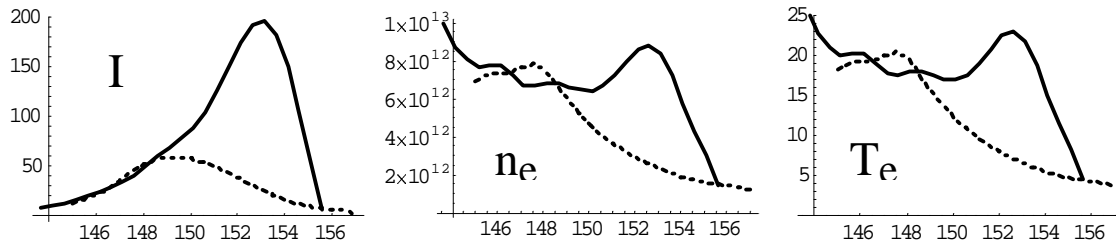


Image plane of the GPI camera . Reconstruction is poor to the lower left ( $I$  and  $n_0$  very small)

## *turbulent (blobby) frame*



## ***comparison of cuts across the frame***



equilibrium dashed, blobby solid

### ***notes***

- cuts normal to the flux surfaces (also see 2D images) suggest that the blob is not completely detached, and has somewhat of a radial streamer character
- intensity appears completely detached because  $n_0$  increases strongly to the right
- the blob or radial streamer in this H-mode data (NSTX #108311) has a characteristic  $n_e \sim 10^{13}/\text{cm}^3$  and  $T_e \sim 25$  eV.

### ***ongoing work***

- compare the properties of the blob (e.g. radial and poloidal velocity, shape and size, rotation and statistics) with theory
  - S.I. Krasheninnikov, Phys. Lett. A 283, 368 (2001); D.A. D'Ippolito, J.R. Myra, S.I. Krasheninnikov, Phys. Plasmas 9, 222 (2002).

# SUMMARY

---

- 3-D DEGAS 2 simulations of GPI reproduce experimental geometry in detail,
- Rough agreement between simulated & observed emission cloud widths,
- But, orientations differ by  $15^\circ$ ,
  - No clear explanation,
  - Could indicate plasma varying on flux surface or problems computing equilibrium.
- Radial resolution not significantly degraded by toroidal extent of cloud.
- DEGAS 2 results provide basis for inferring time-dependent 2-D  $n_e, T_e$  from GPI data.

# REFERENCES

---

- R. J. Maqueda et al., Rev. Sci. Instrum. **74**, 2020 (2002)  
- NSTX GPI description.
- S. J. Zweben et al., Nucl. Fusion, (2003) (to be published)  
- Detailed analysis of NSTX GPI results.
- D. P. Stotler and C. F. F. Karney, Contrib. Plasma Phys. **34**, 392 (1994)  
- Basic DEGAS 2 description.
- D. P. Stotler et al., J. Nucl. Mater. **313–316**, 1066 (2003)  
- DEGAS 2 simulations of C-Mod GPI.
- S. I. Krasheninnikov, Phys. Lett. A **283**, 368 (2001)  
- Basic theory of blobs.

- D. A. D'Ippolito et al., Phys. Plasmas **9**, 222 (2002)  
- Theory of blob motion.
- D. A. D'Ippolito et al., Contrib. Plasma Phys., (2003) (this conference)  
- Ditto.
- M. Goto, J. Quant. Spectrosc. Radiat. Transfer **76**, 331 (2003)  
- He collisional-radiative model.
- P. S. Krstic and D. R. Schultz, J. Phys. B **32**, 3485 (1999)  
- Neutral-ion elastic scattering data.
- S. J. Zweben, et al., Phys. Plasmas **9**, 1981 (2002)  
- Discussion of C-Mod GPI, including DEGAS 2 results.